Multidrug Resistance-Associated Protein 2 (MRP2) Enhances 4-Hydroxynonenal-Induced Toxicity in Madin-Darby Canine Kidney II Cells

ARTICLE *in* CHEMICAL RESEARCH IN TOXICOLOGY · MARCH 2004

Impact Factor: 3.53 · DOI: 10.1021/tx034067m · Source: PubMed

3 AUTHORS, INCLUDING:

Bin Ji
National Institute of Radiological Sciences
44 PUBLICATIONS **782** CITATIONS

SEE PROFILE

Multidrug Resistance-Associated Protein 2 (MRP2) Enhances 4-Hydroxynonenal-Induced Toxicity in Madin−Darby Canine Kidney II Cells

Bin Ji, Kousei Ito, and Toshiharu Horie*

Department of Biopharmaceutics, Graduate School of Pharmaceutical Sciences, Chiba University, Yayoi-cho 1-33, Inage-ku, Chiba, Japan

Received April 2, 2003

4-Hydroxy-*trans*-2,3-nonenal (HNE) is a toxic end product of lipid peroxidation. This multifunctional aldehyde reacts with proteins, phospholipids, and nucleic acids, consequently activating/inactivating enzymes, affecting signal transduction and gene expression. HNE is mainly detoxified by glutathione (GSH) conjugation. In our previous report, we showed that GSH conjugates of 4-hydroxynonenal (HNE-SG) are substrates of multidrug resistance-associated protein 2 (MRP2). MRP2 has been shown to export HNE-SG conjugates into the extracellular space. In the present study, the role of MRP2 in the detoxification of HNE was studied using Madin−Darby canine kidney II (MDCK II) cells expressing human MRP2. MRP2 reduced the intracellular accumulation of HNE-SG conjugate but unexpectedly increased the susceptibility of cells to HNE. The viability of cells was reduced to approximately 70% in the presence of 62.5 μM HNE in MDCK II cells expressing MRP2, whereas MDCK II cells remained unaffected. MRP2 accelerated the elimination of intracellular GSH via a conjugation reaction with HNE (half-life of GSH was 30.1 and 12.2 min for MDCK II cells and MDCK II cells expressing MRP2, respectively). Moreover, the consumption of GSH was unlimited in MDCK II cells expressing MRP2, finally resulting in necrosis. These results indicate that MRP2 has an adverse effect during the detoxification of HNE in MDCK II cells and suggest that expression of MRP2 may enhance the damage caused by oxidative stress.

Introduction

At the time of its discovery in natural fats, 4-hydroxynonenal (HNE) was regarded as a simple byproduct of lipid peroxidation. However, it is now attracting increasing attention. A growing body of evidence suggests that this aldehyde is involved in various biological processes, including growth regulation and differentiation (*1*). In vitro, HNE-induced toxicity is mainly due to the enzyme inactivation of DNA, RNA, and protein synthesis (*2*, *3*). HNE and its protein adducts have also been detected in several diseases (*4*, *5*), suggesting a role for this aldehyde although more studies are need to confirm this.

Three metabolic pathways are involved in the detoxification of HNE. HNE-SG,[1] 1,4-dihydroxynonene, and 4-hydroxynonenoic acid have been identified as primary metabolic products (*6*). Of these metabolites, HNE-SG predominates (*6*−*8*). Although GSH can react with HNE spontaneously, the reaction is accelerated in the presence of GST (*9*).

MRP2 (ABCC2) is a member of the ATP binding cassette (ABC) transport proteins. It is located on the apical domain of polarized cells, such as hepatocytes, enterocytes, and renal tubular cells (*10*−*12*). MRP2 plays an important role in the biliary excretion of some physiological substrates including GSH conjugates, such as GSH disulfide and leukotriene C_4, as well as glucuronide conjugates, such as bilirubin glucuronide and estradiol 17β-D-glucuronide (*13*, *14*). In addition, MRP2 contributes to the drug resistance of cancer cells since it exports a wide range of anticancer drugs from cells on its own or together with GSH (*15*). In a previous study, we demonstrated a role of MRP2 in exporting HNE-SG in in vitro and in vivo experiments (*16*). Active efflux of unmodified xenobiotics has obvious implications for detoxification, while conjugated metabolites are generally thought to be less reactive and already in a "detoxified" state. Thus, it is of great interest to see whether MRP2 can protect cells from HNE-induced cytotoxicity by exporting HNE-SG conjugates. In the present study, MDCK II cells expressing human MRP2 were used to investigate whether MRP2 expression affected HNE-induced cytotoxicity.

Materials and Methods

Materials. HNE was from Cayman Chemical Co. (Ann Arbor, MI). GSH, 2-mercaptoethanol, *o*-phthalaldehyde, and metaphosphoric acid were from Wako Pure Chemical Industries (Osaka, Japan). Monochlorobimane (MCB) was from Molecular Probes (Eugene, OR). GST from equine liver was from Sigma (St. Louis, MO). 3-(4,5-Dimethylthiazol-2-yl)-2,5-diphenyltetrazolium bromide (MTT) was from Acros Organics (Morris Plains, NJ). All other chemicals were of analytical grade.

Preparation and Measurement of HNE-SG Conjugates. HNE-SG conjugates were prepared and measured by the method

* To whom correspondence should be addressed. Tel: 81-43-290-2934. Fax: 81-43-290-3021. E-mail: horieto@p.chiba-u.ac.jp.

[1] Abbreviations: HNE, 4-hydroxy-*trans*-2,3-nonenal; MRP, multidrug resistance-associated protein; GSH, glutathione; HNE-SG, GSH conjugate of HNE; MDCK II, Madin−Darby canine kidney II; MRP2-MDCK II, MDCK II cells expressing the human MRP2; GST, glutathione S-transferase; MCB, monochlorobimane; MTT, 3-(4,5-dimethylthiazol-2-yl)-2,5-diphenyltetrazolium bromide; GS-B, GSH conjugate of monochlorobimane; FBS, fetal bovine serum; PI, propidium iodide; AUC, area under curve; MPT, membrane permeability transition.

10.1021/tx034067m CCC: $27.50
Published on Web 01/10/2004

described in our previous paper (*16*). There are four diastereomeric HNE-SG conjugates formed in the conjugate reaction. The concentration of each conjugate was calculated from the ratio of the height of the respective peak to the total height of these four peaks (*16*). In the present study, HNE-SG is defined as the sum of the four HNE-SG conjugates.

Cell Culture. Wild-type MDCK II cells and MDCK II cells expressing human MRP2 (MRP2-MDCK II) (*17*) were very kindly supplied by Dr. Piet Borst (The Netherlands Cancer Institutes, The Netherlands). Cells were cultured in minimum essential medium Eagle (Sigma) supplemented with 10% FBS at 37 °C in the presence of 5% CO_2. MRP2-MDCK II cells were maintained in the presence of 0.4 mg/mL G418. Cells were seeded in plates with 24 wells at a density of 1.7×10^5 cells per well and cultured for 3 days to form a polarized monolayer in all experiments.

Transport of HNE-SG Conjugates in MDCK II Cells. Cells were washed and incubated at 37 °C with 600 μL of transport buffer (122 mM NaCl, 3 mM KCl, 0.4 mM K_2HPO_4, 1.4 mM $CaCl_2$, 1.2 mM $MgSO_4$, 10 mM Hepes, 25 mM $NaHCO_3$, and 10 mM glucose) containing 50 μM HNE. Aliquots (50 μL) were collected in microtubes containing 100 μL of stop solution (6% metaphosphoric acid and 0.08% EDTA) as samples of the exported HNE-SG. The cells were scraped into 300 μL of stop solution, tapped for 1 min, and centrifuged at 15 000*g* for 5 min. The supernatant was passed through a Millex-LH syringe-driven filter unit (0.45 μm pore size, 4 mm diameter, Millipore Corporation, Billerica, MA) and then subjected to HPLC as a sample of intracellular HNE-SG conjugates. Protein content was determined by the Lowry method (*18*), using bovine serum albumin as standard.

Assay of Cell Viability HNE Treatment. Cells were incubated with FBS-free medium (600 μL) containing different concentrations of HNE. Cell viability was measured 24 h later by MTT assay. Briefly, cells treated with HNE were washed with PBS and incubated with MTT solution (0.5 mg/mL FBS-free medium) for 4 h. MTT formazan formed was dissolved in dimethyl sulfoxide and measured on a Multiskan JX microplate reader (LabSystems, Altrincham, U.K.) with 630 and 570 nm as reference and test wavelengths, respectively.

Assessment of Form of Cell Death. The form of cell death was assessed using an Annexin V-EGFP Apoptosis Detection Kit (BioVision, Inc., Mountain View, CA). Cells were seeded onto glass coverslips coated with collagen in a 24 well plate at a density of 1.7×10^5 cells per well and cultured for 3 days to form monolayers. The cells were washed with PBS at different times after incubation with HNE in FBS-free medium and then incubated with binding buffer containing annexin V-EGFP and PI at room temperature for 5 min in the dark. Coverslips were inverted and visualized using an LSM510 confocal laser scanning microscope (Carl Zeiss, Jena, Germany). The 488 nm wavelength line of an argon laser and the 546 nm wavelength line of a helium−neon laser were used with appropriate combinations of excitation and emission filters.

Assay of Intracellular ATP and GSH. Cells were incubated with FBS-free medium (600 μL) containing HNE (62.5 μM). Cells were then harvested in 0.5 mL of 3% $HClO_4$ and disrupted by vortex mixing. After they were neutralized with 1 N KOH, samples were centrifuged at 15 000*g* for 30 s and the supernatants were used for the ATP assay. The cellular ATP content was measured with an ATP bioluminescent assay kit (Sigma) based on the luciferin−luciferase method using a TD-20/20 luminometer (Turner Designs, Sunnyvale, CA). To measure the intracellular GSH, cells were harvested into stop solution and then disrupted by vortex mixing for 1 min and centrifuged at 15 000*g* for 5 min. The supernatant was passed through a Millex-LH syringe-driven filter unit and then directly injected onto the HPLC column. A postlabel HPLC system was used according to a previous report (*19*). Briefly, an Inertsil ODS column (4.6 mm inner diameter × 250 mm, GL Sciences Ltd., Tokyo, Japan) was used and elution was carried out with mobile phase (11% methanol in H_2O containing 0.1% trifluoroacetic acid) at flow rate of 1.0 mL/min. The eluate from the column was mixed with reagent solution containing 2.3 mM *o*-phthalaldehyde and 17.1 mM 2-mercaptoethanol in 100 mM carbonate buffer (pH 10.5) delivered at 0.2 mL/min. The mixture was then passed through a stainless steel coil at 70 °C to facilitate derivatization. A fluorescence detector was operated at an excitation and emission wavelength of 355 and 425 nm, respectively.

Assay of GST Activity. The cytosolic GST of MDCK II cells was determined by the method described previously (*20*). Briefly, cells were scraped and homogenized in 50 mM Tris-HCl buffer (pH 6.8) and centrifuged at 20 800*g* for 45 min. The supernatants were used as cytosolic samples. Reaction mixtures in potassium phosphate buffer (pH 6.5) consisted of cytosol (0.2 mg protein/mL), GSH (400 μM), and MCB (5 μM). The production of GS-B was monitored using an F-2000 fluorescence spectrophotometer (Hitachi, Tokyo, Japan) with excitation and emission wavelengths of 386 and 476 nm, respectively, after starting reactions with the addition of MCB.

Statistical Analysis. Statistical analyses were performed by Student's *t*-test or ANOVA followed by a post hoc test (Bonferroni) as described in the legends. Differences were considered to be statistically significant if $p < 0.05$.

Results

Formation and Transport of HNE-SG Conjugates in MDCK II/MRP2-MDCK II Cells. Export of HNE-SG conjugates in MRP2-MDCK II cells was significantly higher than that in MDCK II cells (Figure 1A). In contrast, the amount of intracellular HNE-SG conjugates in MDCK II cells was approximately 5-fold higher than that in MRP2-MDCK II cells (Figure 1B). The total amount of HNE-SG conjugates formed in MRP2-MDCK II cells, defined as the sum of those exported and remaining in the cells, was approximately 2-fold higher than that in MDCK II cells (Figure 1C).

HNE-Induced Cytotoxicity in MDCK II and MRP2-MDCK II Cells. The viability of cells 24 h after HNE treatment was measured by MTT assay. Unexpectedly, the expression of MRP2 enhanced HNE-induced cytotoxicity in MDCK II cells. The viability of cells was reduced to approximately 70% in the presence of 62.5 μM HNE in MRP2-MDCK II cells, whereas MDCK II cells remained unaffected. In the presence of a higher concentration of HNE (from 125 to 500 μM), all MRP2-MDCK II cells were killed, while the viability of MDCK II cells was gradually reduced from 60 to 20% (Figure 2).

Assessment of the Type of Cell Death. Dead cells were scarcely detected in MDCK II cells even after cells were incubated with 62.5 μM HNE for 24 h. In contrast, necrotic cells (annexin V negative and PI uptake positive) appeared 12 h later after 62.5 μM HNE treatment in MRP2-MDCK II cells. A higher concentration (250 μM) of HNE induced necrosis in both types of cell (Figure 3). In addition, nucleosomal fragmentation and chromatin condensation were not observed (data not shown). Thus, HNE induced necrosis rather than apoptosis in these cells.

Intracellular GSH Depletion after HNE Treatment in MDCK II/MRP2-MDCK II Cells. A slight reduction in the initial GSH level was observed in MRP2-MDCK II cells as compared with MDCK II cells (18.0 ± 1.9 vs 22.1 ± 1.2 nmol/mg protein) as reported previously (*21*). The intracellular GSH content was rapidly reduced in both cells after HNE addition. The elimination rate constant calculated from the initial three points (0, 10, and 30 min) was enhanced in MRP2-MDCK II cells (0.057 min^{-1}, $t_{1/2} = 12.2$ min) as compared with MDCK II cells

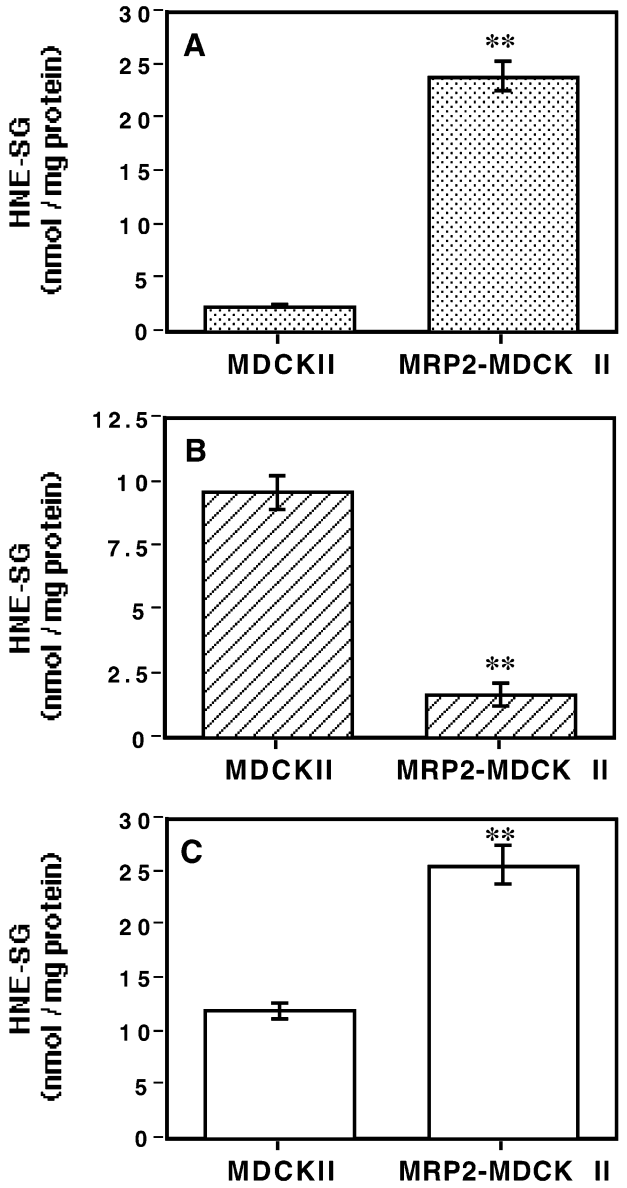

Figure 1. Export and intracellular accumulation of HNE-SG conjugates in MDCK II and MRP2-MDCK II cells. The cell monolayers were incubated in the presence of HNE (50 μM) for 12 min. The amount of extracellular and intracellular HNE-SG conjugates was determined as described in the Materials and Methods. (A) Export of HNE-SG conjugates, (B) intracellular accumulation of HNE-SG conjugates, and (C) formation (sum of export and intracellular accumulation) of HNE-SG conjugates. Results are given as the mean ± SEM of three independent experiments. **$p < 0.01$ significantly different from MDCK II cells, Student's *t*-test.

($0.023\ min^{-1}$, $t_{1/2} = 30.1$ min) (Figure 4). The intracellular GSH in MRP2-MDCK II cells was almost completely depleted 30 min later (approximately 2% of the initial level), while that in MDCK II cells was reduced to approximately 25% of initial level and thereafter remained stable (Figure 4). The AUC values calculated from the initial 4 h were 15.4 ± 1.3 and 3.6 ± 0.6 nmol h/mg for MDCK II and MRP2-MDCK II cells, respectively ($p < 0.01$, significant difference, $n = 3$, Student's *t*-test). The GSH content of MDCK II cells returned to the initial level 24 h later, while that of MRP2-MDCK II cells did not (Figure 4). The partial recovery of the GSH content of MRP2-MDCK II cells at 24 h might be due to the residual cells surviving the HNE treatment. This is consistent with the MTT assay shown in Figure 2, where 65% of MRP2-MDCK II cells were still alive after a 24 h of treatment with 62.5 μM HNE. The intramitochondrial GSH content of MDCK II cells was reduced to 20% of the initial level at 30 min after HNE addition and maintained thereafter, while that in MRP2-MDCK II cells fell to an undetectable level (data not shown). This profile is very similar to that of intracellular GSH, suggesting that intramitochondrial GSH is depleted by HNE in parallel with intracellular GSH.

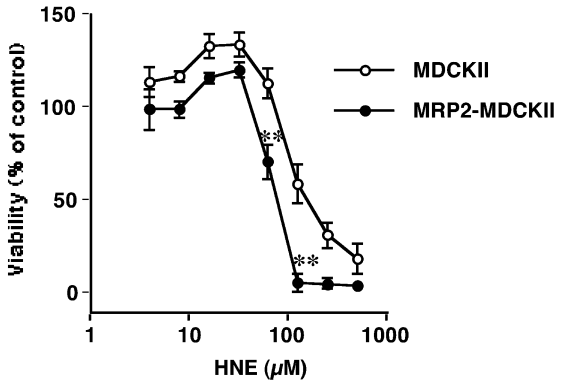

Figure 2. Viability of cells treated with HNE. The cell monolayers were incubated with FBS-free medium at 37 °C in the presence of the indicated concentration of HNE for 24 h as described in the Materials and Methods. Viability of cells was measured by MTT assay. Results are given as the mean ± SEM of four independent experiments. **$p < 0.01$ significantly different from MDCK II cells, ANOVA followed by Bonferroni.

Inhibitory Effect of HNE-SG on the GST Activity of MDCK II Cells. Because S-alkyl derivatives of GSH are good inhibitors of GST (*22*), HNE-SG likely caused progressive inhibition as it was being formed. There was no difference in GST activity between MDCK II and MRP2-MDCK II cells using GS-B as a substrate (data not shown). Cytosolic GST activity was inhibited approximately 50% in the presence of 50 μM HNE-SG conjugates (Figure 5).

Intracellular ATP Levels after Treatment of Cells with HNE. The intracellular ATP levels were not reduced to lethal low levels over 12 h following the addition of HNE to both types of cells. After 24 h, the ATP level was reduced to approximately 30% of the initial level in MRP2-MDCK II cells, whereas there was no significant change in MDCK II cells (Figure 6). Thus, the loss of ATP in MRP2-MDCK II cells was likely a consequence of cell death rather than the cause of necrosis.

Discussion

HNE induces necrosis and/or apoptosis in many cell lines (*23*−*27*). Mitochondrial dysfunction is suggested to be responsible for HNE-induced cell death (*24*, *25*, *27*). The mitochondrion is a major organelle releasing reactive oxygen species, and the mitochondrial antioxidant system is dependent on intramitochondrial GSH and GSH peroxidase. GSH depletion induces mitochondrial permeability transition (MPT) and sequent necrosis or apoptosis (*28*, *29*). Mitochondrial damage may play a role in HNE-induced cell death, considering our experimental results and the following facts: (i) HNE can induce MPT (*27*); (ii) GSH depletion impairs mitochondrial function and triggers MPT (*30*, *31*); and (iii) GSH may be necessary for apoptosis because GSH depletion converts death

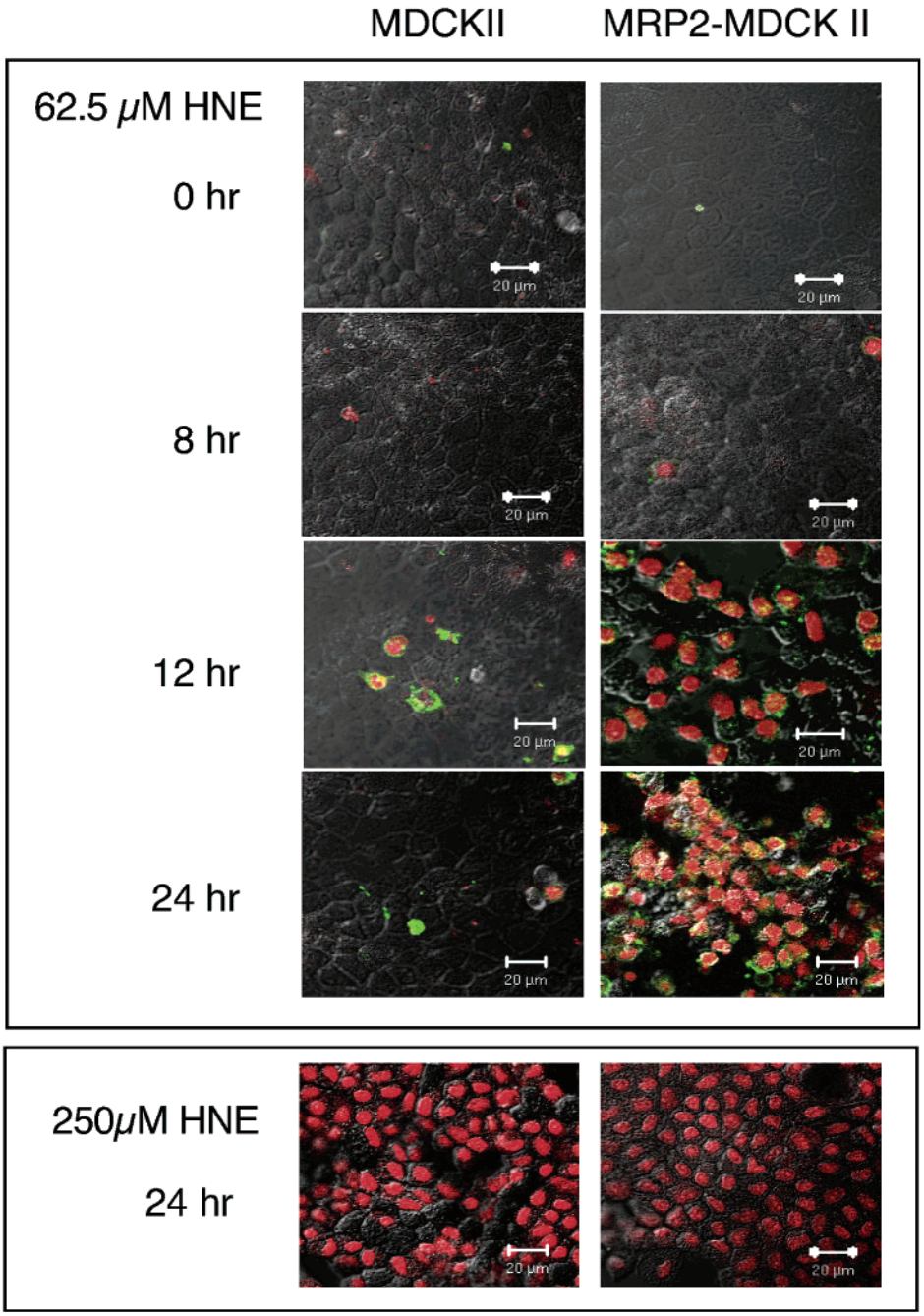

Figure 3. PI uptake and annexin V binding after HNE treatment. The cell monolayers were washed with PBS 0, 8, 12, and 24 h after incubation with the indicated concentration of HNE. The cells were then incubated with binding buffer containing annexin V-EGFP (green) and PI (red) at room temperature for 5 min in the dark and then observed under a confocal laser scanning microscope. Left panel, MDCK II; right panel, MRP2-MDCK II.

receptor-mediated apoptosis to necrosis (*32*, *33*). It is conceivable that HNE depletes intracellular GSH including mitochondrial GSH, therefore inducing oxidative stress and MPT, subsequently resulting in necrosis. MRP2 accelerates the depletion of intracellular GSH and hence enhances HNE-induced cytotoxicity in MRP2-MDCK II cells. Similarly, MRP2-MDCK II cells can be killed off by ethacrynic acid (125 μM), which exerts its toxicity by inducing depletion of intracellular GSH and lipid peroxidation (*34*), while parent MDCK II cells treated with the same concentration remain alive (unpublished data).

GST effectively catalyzes the conjugation reaction of HNE with GSH (*1*, *9*, *35*). GST activity toward MCB was inhibited by 50% in the presence of 50 μM HNE-SG (Figure 5). Alin et al. reported a strong inhibitory effect of HNE (IC_{50} of 5 μM) on rat GST 4-4 activity with 1-chloro-2,4-dinitrobenzene as the electrophilic substrate (*35*). Because the GST isoenzymes catalyzing the conjugation of HNE with GSH are not identified in MDCK II cells, we were unable to conclude whether the GST isoenzyme catalyzing conjugation of MCB with GSH is also responsible for the conjugation of HNE. However, most of the GST isoenzymes tested show a degree of catalytic activity in the conjugation of HNE with GSH (*35*, *36*) and reversible inhibition byproducts are well-known (*22*), so that accumulation of intracellular HNE-SG may reduce the formation of HNE-SG and subsequent

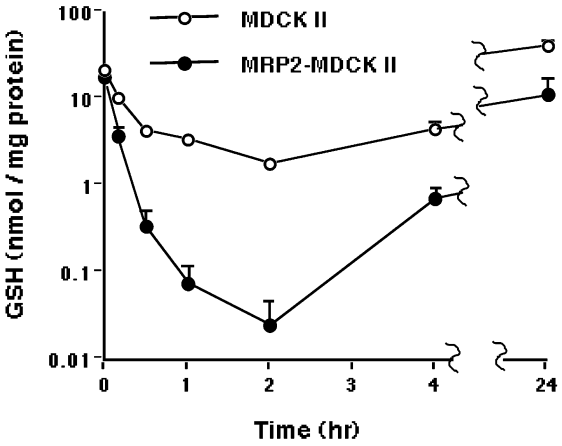

Figure 4. GSH depletion in MDCK II and MRP2-MDCK II cells treated with HNE. The cell monolayers were incubated in FBS-free medium in the presence of HNE (62.5 μM) for the indicated time. Intracelluar GSH was measured as described in the Materials and Methods. Results are given as the mean ± SEM of three independent experiments.

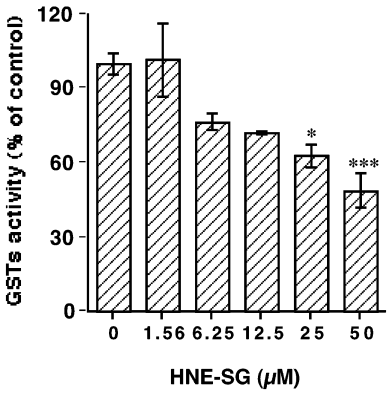

Figure 5. HNE-SG conjugates inhibited the activity of cytosolic GST of MDCK II cells in vitro. The activity of GST was evaluated using the rate of GS-B formation. Reaction mixtures consisted of cytosol (0.2 mg/mL), GSH (400 μM), and MCB (5 μM) in potassium phosphate buffer (pH 6.5). GS-B formation was monitored by a fluorescence spectrophotometer with excitation and emission wavelengths of 386 and 476 nm, respectively. Results are given as the mean ± SEM of three independent experiments. *$p < 0.05$ and ***$p < 0.001$ significantly different from data in the absence of HNE-SG, ANOVA followed by Bonferroni.

consumption of GSH. Actually, intracellular HNE-SG at 12 min after 50 μM HNE treatment (Figure 1) was calculated to be 2 and 0.33 mM for MDCK II and MRP2-MDCK II cells, respectively [cell volume was calculated using the assumption that 1 mg of protein equals 5 μL of volume (2.1×10^6 cells ≒ 1 mg protein in MDCK II cells, and the volume of one MDCK cell is approximately 2.5 pL; *37*)]. An approximately 7-fold higher intracellular HNE-SG concentration in MDCK II cells seems to produce stronger product inhibition than that in MRP2-MDCK II cells. Mice lacking GST π show an increased resistance to acetaminophen-induced hepatotoxicity (*38*). As GSH depletion and subsequent oxidative stress are involved in acetaminophen-induced hepatotoxicity (*39*), GST may increase cellular injury by accelerating GSH consumption. Thus, inhibition of GST by intracellular HNE-SG may contribute to the attenuation of HNE-induced cytotoxicity in MDCK II cells.

The protective role of MRPs against toxins is well-known. Expression of MRPs confers resistance to anti-

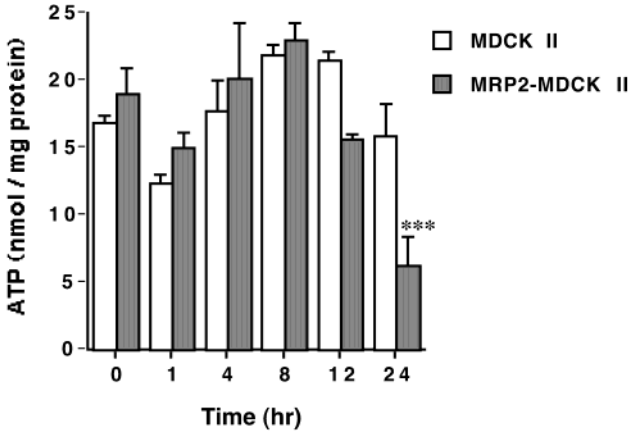

Figure 6. Intracellular ATP level. The cell monolayers were incubated with HNE (62.5 μM) at 37 °C. Intracellular ATP was measured at the indicated times as described in the Materials and Methods. Results are given as the mean ± SEM of three independent experiments. ***$p < 0.001$ significantly different from the data in MRP2-MDCK II cells before the addition of HNE (0 h), ANOVA followed by Bonferroni.

cancer drugs and heavy metals in cells in a GSH-dependent or -independent manner (*40*). Importantly, conjugation of GSH with a hydrophobic moiety dramatically increases transport affinity for MRP2 as demonstrated with conjugates of 2,4-dinitrophenyl (DNP-SG) ($K_m \sim 80$ μM) and leukotriene A_4 (LTC_4) ($K_i \sim 0.65$ μM) (*41*) as compared with GSH itself ($K_m \sim 15$ mM) (*21*). Such cooperative action of GST and MRP2 has been widely accepted as being a defense mechanism (*22*, *42*). However, that converse situation aggravates acute cytotoxicity under particularly severe oxidative stress as shown in this study and a previous report (*43*). In the present study, expression of MRP2 rather enhanced HNE-induced acute cytotoxicity in MDCK II cells as accumulation of HNE-SG in MDCK II was not toxic to the cells (i.e., HNE seemed already detoxified by conjugation with GSH). Severe GSH depletion-induced necrosis is the likely mechanism of HNE-induced toxicity in our case. This suggests a harmful role for MRP2 in defending against oxidative stress. This view is indirectly supported by previous in vivo experiments: (i) MRP2 deficient TR^- rat is protected from cholestasis induced by α-naphthylisothiocyanate, which exerts its toxicity by depleting cellular GSH (*43*), and (ii) cholestatic rats with bile duct ligation are protected from acetaminophen-induced hepatic injury (*44*). Independently, bile duct ligation down regulates the expression of MRP2 protein and localization on the canalicular membrane (*45*). Although it was not measured, preserved GSH might partly involved in the attenuation of acetaminophen-induced hepatic injury in bile duct ligated rats (*44*). The physiological significance of the internalization and down regulation of MRP2 by several oxidative stress-inducing compounds or treatments (*46*−*48*) could be considered as a feedback mechanism to maintain intracellular GSH.

Acknowledgment. We thank Dr. Piet Borst (The Netherlands Cancer Institute, Amsterdam, The Netherlands) for kindly supplying MDCK II cells expressing human MRP2. This work was supported in part by a Grant-in-Aid for Scientific Research from The Ministry of Education, Culture, Sports, Science and Technology of Japan.

References

(1) Esterbauer, H., Schaur, R. J., and Zollner, H. (1991) Chemistry and biochemistry of 4-hydroxynonenal, malonaldehyde and related aldehydes. *Free Radical Biol. Med. 11*, 81−128.

(2) Poli, G., Albano, E., and Dianzani, M. U. (1987) The role of lipid peroxidation in liver damage. *Chem. Phys. Lipids 45*, 117−142.

(3) Keller, J. N., Pang, Z., Geddes, J. W., Begley, J. G., Germeyer, A., Waeg, G., and Mattson, M. P. (1997) Impairment of glucose and glutamate transport and induction of mitochondrial oxidative stress and dysfunction in synaptosomes by amyloid beta-peptide: role of the lipid peroxidation product 4- hydroxynonenal. *J. Neurochem. 69*, 273−284.

(4) Paradis, V., Kollinger, M., Fabre, M., Holstege, A., Poynard, T., and Bedossa, P. (1997) In situ detection of lipid peroxidation byproducts in chronic liver diseases. *Hepatology 26*, 135−142.

(5) Chen, J., Robinson, N. C., Schenker, S., Frosto, T. A., and Henderson, G. I. (1999) Formation of 4-hydroxynonenal adducts with cytochrome *c* oxidase in rats following short-term ethanol intake. *Hepatology 29*, 1792−1798.

(6) Boon, P. J., Marinho, H. S., Oosting, R., and Mulder, G. J. (1999) Glutathione conjugation of 4-hydroxy-*trans*-2,3-nonenal in the rat in vivo, the isolated perfused liver and erythrocytes. *Toxicol. Appl. Pharmacol. 159*, 214−223.

(7) Ishikawa, T., Esterbauer, H., and Sies, H. (1986) Role of cardiac glutathione transferase and of the glutathione S- conjugate export system in biotransformation of 4-hydroxynonenal in the heart. *J. Biol. Chem. 261*, 1576−1581.

(8) Grune, T., Siems, W. G., and Petras, T. (1997) Identification of metabolic pathways of the lipid peroxidation product 4-hydroxynonenal in in situ perfused rat kidney. *J. Lipid Res. 38*, 1660−1665.

(9) Goon, D., Saxena, M., Awasthi, Y. C., and Ross, D. (1993) Activity of mouse liver glutathione S-transferases toward *trans*,*trans*-muconaldehyde and *trans*-4-hydroxy-2-nonenal. *Toxicol. Appl. Pharmacol. 119*, 175−180.

(10) Schaub, T. P., Kartenbeck, J., Konig, J., Vogel, O., Witzgall, R., Kriz, W., and Keppler, D. (1997) Expression of the conjugate export pump encoded by the mrp2 gene in the apical membrane of kidney proximal tubules. *J. Am. Soc. Nephrol. 8*, 1213−1221.

(11) Kartenbeck, J., Leuschner, U., Mayer, R., and Keppler, D. (1996) Absence of the canalicular isoform of the MRP gene-encoded conjugate export pump from the hepatocytes in Dubin-Johnson syndrome. *Hepatology 23*, 1061−1066.

(12) Mottino, A. D., Hoffman, T., Jennes, L., and Vore, M. (2000) Expression and localization of multidrug resistant protein mrp2 in rat small intestine. *J. Pharmacol. Exp. Ther. 293*, 717−723.

(13) Keppler, D., and Konig, J. (1997) Hepatic canalicular membrane 5: Expression and localization of the conjugate export pump encoded by the MRP2 (cMRP/cMOAT) gene in liver. *FASEB J. 11*, 509−516.

(14) Suzuki, H., and Sugiyama, Y. (1998) Excretion of GSSG and glutathione conjugates mediated by MRP1 and cMOAT/MRP2. *Semin. Liver Dis. 18*, 359−376.

(15) Konig, J., Nies, A. T., Cui, Y., Leier, I., and Keppler, D. (1999) Conjugate export pumps of the multidrug resistance protein (MRP) family: localization, substrate specificity, and MRP2-mediated drug resistance. *Biochim. Biophys. Acta 1461*, 377−394.

(16) Ji, B., Ito, K., Suzuki, H., Sugiyama, Y., and Horie, T. (2002) Multidrug resistance-associated protein2 (MRP2) plays an important role in the biliary excretion of glutathione conjugates of 4-hydroxynonenal. *Free Radical Biol. Med. 33*, 370−378.

(17) Evers, R., Kool, M., van Deemter, L., Janssen, H., Calafat, J., Oomen, L. C., Paulusma, C. C., Oude Elferink, R. P., Baas, F., Schinkel, A. H., and Borst, P. (1998) Drug export activity of the human canalicular multispecific organic anion transporter in polarized kidney MDCK cells expressing cMOAT (MRP2) cDNA. *J. Clin. Invest. 101*, 1310−1319.

(18) Lowry, O. H., Rosebrough, N. J., Farr, A. L., and Randall, R. J. (1951) Protein measurement with the folin phenol reagent. *J. Biol. Chem. 193*, 265−275.

(19) Keller, D. A., and Menzel, D. B. (1985) Picomole analysis of glutathione, glutathione disulfide, glutathione S-sulfonate, and cysteine S-sulfonate by high-performance liquid chromatography. *Anal. Biochem. 151*, 418−423.

(20) He, N. G., Singhal, S. S., Chaubey, M., Awasthi, S., Zimniak, P., Partridge, C. A., and Awasthi, Y. C. (1996) Purification and characterization of a 4-hydroxynonenal metabolizing glutathione S-transferase isozyme from bovine pulmonary microvessel endothelial cells. *Biochim. Biophys. Acta 1291*, 182−188.

(21) Paulusma, C. C., van Geer, M. A., Evers, R., Heijn, M., Ottenhoff, R., Borst, P., and Oude Elferink, R. P. (1999) Canalicular multispecific organic anion transporter/multidrug resistance protein 2 mediates low-affinity transport of reduced glutathione. *Biochem. J. 338*, 393−401.

(22) van Bladeren, P. J. (2000) Glutathione conjugation as a bioactivation reaction. *Chem.-Biol. Interact. 129*, 61−76.

(23) Herbst, U., Toborek, M., Kaiser, S., Mattson, M. P., and Hennig, B. (1999) 4-Hydroxynonenal induces dysfunction and apoptosis of cultured endothelial cells. *J. Cell Physiol. 181*, 295−303.

(24) Ji, C., Amarnath, V., Pietenpol, J. A., and Marnett, L. J. (2001) 4-hydroxynonenal induces apoptosis via caspase-3 activation and cytochrome *c* release. *Chem. Res. Toxicol. 14*, 1090−1096.

(25) Kruman, II, and Mattson, M. P. (1999) Pivotal role of mitochondrial calcium uptake in neural cell apoptosis and necrosis. *J. Neurochem. 72*, 529−540.

(26) Nakajima, A., Yamada, K., Zou, L. B., Yan, Y., Mizuno, M., and Nabeshima, T. (2002) Interleukin-6 protects PC12 cells from 4-hydroxynonenal-induced cytotoxicity by increasing intracellular glutathione levels. *Free Radical Biol. Med. 32*, 1324−1332.

(27) Vieira, H. L., Belzacq, A. S., Haouzi, D., Bernassola, F., Cohen, I., Jacotot, E., Ferri, K. F., El Hamel, C., Bartle, L. M., Melino, G., Brenner, C., Goldmacher, V., and Kroemer, G. (2001) The adenine nucleotide translocator: a target of nitric oxide, peroxynitrite, and 4-hydroxynonenal. *Oncogene 20*, 4305−4316.

(28) Armstrong, J. S., and Jones, D. P. (2002) Glutathione depletion enforces the mitochondrial permeability transition and causes cell death in Bcl-2 overexpressing HL60 cells. *FASEB J. 16*, 1263−1265.

(29) Lemasters, J. J., Nieminen, A. L., Qian, T., Trost, L. C., Elmore, S. P., Nishimura, Y., Crowe, R. A., Cascio, W. E., Bradham, C. A., Brenner, D. A., and Herman, B. (1998) The mitochondrial permeability transition in cell death: a common mechanism in necrosis, apoptosis and autophagy. *Biochim. Biophys. Acta 1366*, 177−196.

(30) Kowaltowski, A. J., Castilho, R. F., and Vercesi, A. E. (2001) Mitochondrial permeability transition and oxidative stress. *FEBS Lett. 495*, 12−15.

(31) Jha, N., Jurma, O., Lalli, G., Liu, Y., Pettus, E. H., Greenamyre, J. T., Liu, R. M., Forman, H. J., and Andersen, J. K. (2000) Glutathione depletion in PC12 results in selective inhibition of mitochondrial complex I activity. Implications for Parkinson's disease. *J. Biol. Chem. 275*, 26096−26101.

(32) Haouzi, D., Lekehal, M., Tinel, M., Vadrot, N., Caussanel, L., Letteron, P., Moreau, A., Feldmann, G., Fau, D., and Pessayre, D. (2001) Prolonged, but not acute, glutathione depletion promotes Fas-mediated mitochondrial permeability transition and apoptosis in mice. *Hepatology 33*, 1181−1188.

(33) Hentze, H., Gantner, F., Kolb, S. A., and Wendel, A. (2000) Depletion of hepatic glutathione prevents death receptor-dependent apoptotic and necrotic liver injury in mice. *Am. J. Pathol. 156*, 2045−2056.

(34) Yamamoto, K., Masubuchi, Y., Narimatsu, S., Kobayashi, S., and Horie, T. (2002) Toxicity of ethacrynic acid in isolated rat hepatocytes. *Toxicol. In Vitro 16*, 151−158.

(35) Alin, P., Danielson, U. H., and Mannervik, B. (1985) 4-Hydroxyalk-2-enals are substrates for glutathione transferase. *FEBS Lett. 179*, 267−270.

(36) Hubatsch, I., Ridderstrom, M., and Mannervik, B. (1998) Human glutathione transferase A4-4: an alpha class enzyme with high catalytic efficiency in the conjugation of 4-hydroxynonenal and other genotoxic products of lipid peroxidation. *Biochem. J. 330*, 175−179.

(37) Mills, J. W., and Lubin, M. (1986) Effect of adenosine 3′,5′-cyclic monophosphate on volume and cytoskeleton of MDCK cells. *Am. J. Physiol. 250*, C319−C324.

(38) Henderson, C. J., Wolf, C. R., Kitteringham, N., Powell, H., Otto, D., and Park, B. K. (2000) Increased resistance to acetaminophen hepatotoxicity in mice lacking glutathione S-transferase Pi. *Proc. Natl. Acad. Sci. U.S.A. 97*, 12741−12745.

(39) Lores Arnaiz, S., Llesuy, S., Cutrin, J. C., and Boveris, A. (1995) Oxidative stress by acute acetaminophen administration in mouse liver. *Free Radical Biol. Med. 19*, 303−310.

(40) Leslie, E. M., Deeley, R. G., and Cole, S. P. (2001) Toxicological relevance of the multidrug resistance protein 1, MRP1 (ABCC1) and related transporters. *Toxicology 167*, 3−23.

(41) Ito, K., Suzuki, H., and Sugiyama, Y. (2001) Charged amino acids in the transmembrane domains are involved in the determination of the substrate specificity of rat Mrp2. *Mol. Pharmacol. 59*, 1077−1085.

(42) Paumi, C. M., Ledford, B. G., Smitherman, P. K., Townsend, A. J., and Morrow, C. S. (2001) Role of multidrug resistance protein 1 (MRP1) and glutathione S-transferase A1-1 in alkylating agent resistance. Kinetics of glutathione conjugate formation and efflux govern differential cellular sensitivity to chlorambucil versus melphalan toxicity. *J. Biol. Chem. 276*, 7952−7956.

(43) Dietrich, C. G., Ottenhoff, R., de Waart, D. R., and Oude Elferink, R. P. (2001) Role of MRP2 and GSH in intrahepatic cycling of toxins. *Toxicology 167*, 73−81.

(44) Acevedo, C., Bengochea, L., Tchercansky, D. M., Ouvina, G., Perazzo, J. C., Lago, N., Lemberg, A., and Rubio, M. C. (1995) Cholestasis as a liver protective factor in paracetamol acute overdose. *Gen. Pharmacol. 26*, 1619−1624.

(45) Paulusma, C. C., Kothe, M. J., Bakker, C. T., Bosma, P. J., van Bokhoven, I., van Marle, J., Bolder, U., Tytgat, G. N., and Oude Elferink, R. P. (2000) Zonal down-regulation and redistribution of the multidrug resistance protein 2 during bile duct ligation in rat liver. *Hepatology 31*, 684−693.

(46) Schmitt, M., Kubitz, R., Wettstein, M., vom Dahl, S., and Haussinger, D. (2000) Retrieval of the mrp2 gene encoded conjugate export pump from the canalicular membrane contributes to cholestasis induced by *tert*-butyl hydroperoxide and chloro-dinitrobenzene. *Biol. Chem. 381*, 487−495.

(47) Kubitz, R., Wettstein, M., Warskulat, U., and Haussinger, D. (1999) Regulation of the multidrug resistance protein 2 in the rat liver by lipopolysaccharide and dexamethasone. *Gastroenterology 116*, 401−410.

(48) Zhang, C., Walker, L. M., Hinson, J. A., and Mayeux, P. R. (2000) Oxidant stress in rat liver after lipopolysaccharide administration: effect of inducible nitric-oxide synthase inhibition. *J. Pharmacol. Exp. Ther. 293*, 968−972.

TX034067M